


## SIMULATION OF TUNNEL DIODE I–V CHARACTERISTICS WITH PHOTOCURRENT AND PHONON-ASSISTED PROCESSES

 Mukhammadjon G. Dadamirzaev<sup>1</sup>,  Munirakhon K. Uktamova<sup>1,2</sup>, Shirin Rakhmanova<sup>3</sup>, Gayrat A. Ibadullayev<sup>4</sup>

<sup>1</sup>Namangan State Technical University, 160103 Namangan, Uzbekistan

<sup>2</sup>University of Business and Science, Uzbekistan

<sup>3</sup>Urgench State University, Uzbekistan

<sup>4</sup>Urgench State Pedagogical Institute, Uzbekistan

\*Corresponding author: [umk9391@gmail.com](mailto:umk9391@gmail.com)

Received September 2, 2025; accepted November 23, 2025

In this paper, a unified current model for tunnel diodes has been developed. The model incorporates not only the tunneling, diffusion, and excess currents but also the photocurrent generated under illumination. In addition, phonon-assisted tunneling processes, namely phonon absorption and phonon emission, arising from electron–phonon interactions, have been included. The calculated current–voltage characteristics indicate that the total current shifts downward under illumination. It is demonstrated that the photocurrent increases proportionally with the optical intensity and wavelength. In the case of phonon absorption, electrons gain additional energy, the tunneling channel broadens, and the peak current increases by approximately 15–20%. Conversely, during phonon emission, part of the electron energy is lost, reducing the tunneling probability, and the peak current decreases by about 10–12%. The obtained results indicate that accounting for phonon and photon processes significantly extends the application potential of tunnel diodes in optoelectronic and photodetector devices. The proposed model provides a theoretical basis for the development of tunnel diodes as high-frequency, light-sensitive, and energy-efficient devices.

**Keywords.** Tunnel diode; Photocurrent; Diffusion current; Excess current; Semiconductor modeling; Phonon-assisted tunneling; Optoelectronic devices

**PACS:** 42.66

### INTRODUCTION

Researchers have developed a wide range of models to describe the current–voltage (I–V) characteristics of tunnel diodes. Regardless of their diversity, a reliable tunneling model must accurately reproduce three essential features: (i) the peak current regime, where tunneling dominates; (ii) the valley current regime, where the tunneling probability decreases, and drift mechanisms begin to prevail; and (iii) the diode regime, where carrier drift and diffusion dominate [1]. In the classical Tsu–Esaki model, several of these phenomena are captured, but excess and diffusion currents are not fully incorporated. Later, O. Kan demonstrated that the tunneling current strongly depends on the density of states and on the Wenzel–Kramers–Brillouin (WKB) approximation applied to parabolic and non-parabolic electron transitions [2]. The model proposed by Karlovsky, based on the Franz–Keldysh effect, offered a more straightforward approach for evaluating the current in tunnel diodes but considered only the band bending in the semiconductor’s *n*-region [3,4]. Yajima and Esaki discussed the concept of excess current, while Chynoweth [5] proposed a more complete description. Subsequent studies extended these foundations by including additional mechanisms such as generation–recombination processes, illumination-induced photocurrents, and phonon-assisted tunneling (PAT). Under classical tunneling conditions, electron energies must coincide exactly. However, as Tien and Gordon established, phonon interactions significantly modify tunneling, especially in the presence of external electromagnetic fields. Phonon absorption and emission create *satellite tunneling channels*, enriching the I–V characteristics and producing complex behavior under illumination [6]. Recent investigations have further advanced the theoretical and experimental understanding of these effects. Liu et al. proposed an analytical framework that refines tunneling current density calculations by incorporating nonparabolic band structures [9]. Février et al. demonstrated the influence of photon-assisted transport and coherent tunneling in nanoscale junctions, linking optical excitation with negative differential resistance phenomena [10]. Mendez et al. provided detailed *ab initio* simulations of phonon coupling under high-field and quantum confinement conditions, emphasizing the interplay between lattice vibrations and electron tunneling [11]. Similarly, Sugiura et al. investigated tunnel mechanisms in semiconductor devices designed for renewable energy applications, revealing how energy-band engineering can enhance tunneling efficiency [12]. Additionally, Moulin revisited the I–V characteristics of *p–n* tunnel junctions and proposed a revised semi-empirical model that aligns well with experimental data for homojunctions [13]. These studies collectively highlight the growing attention to photon- and phonon-assisted processes and their critical roles in shaping the nonlinear response of tunnel junctions. Nevertheless, existing models still treat these mechanisms separately and rarely unify all contributions—including direct tunneling, diffusion, excess, phonon-assisted, and photo-induced currents—within a single analytical framework.

Therefore, in this work, we present a comprehensive current model for tunnel diodes that explicitly includes photocurrent generation and phonon-assisted tunneling, providing a unified description of the total current in illuminated and non-illuminated conditions. This approach aims to bridge the gap between earlier theoretical models and recent experimental findings, contributing to a deeper understanding of quantum transport in nonlinear semiconductor structures.

## METHODS

The hole and electron energies at the p–n junction in tunnel diodes  $f_1(\varepsilon_1)$  and  $f_2(\varepsilon_2)$  are the Fermi–Dirac distribution functions for holes and electrons in the p and n-regions of the semiconductor, and their difference takes the form:  $f_1(\varepsilon_1) - f_2(\varepsilon_2) = \frac{1}{\exp(\frac{\varepsilon - \mu_n}{kT}) + 1} - \frac{1}{\exp(\frac{\varepsilon - \mu_n + qV}{kT}) + 1}$ . The Wentzel–Kramers–Brillouin (WKB) approximation provides an analytical framework for describing quantum tunneling through a slowly varying potential barrier. In this method, the stationary one-dimensional Schrödinger equation for an electron of energy  $E$  moving in a potential  $V(x)$  is written as

$$\frac{d^2\psi(x)}{dx^2} + \frac{2m}{\hbar^2} [E - V(x)]\psi(x) = 0 \quad (1)$$

Introducing the local wave number  $k(x) = \sqrt{\frac{2m}{\hbar^2} |E - V(x)|}$  the WKB solution can be expanded as an  $\hbar^2$ -series of the exponential form

$$\psi(x) = \exp\left[\frac{i}{\hbar} S(x)\right] S(x) = S_0(x) + \frac{\hbar}{i} S_1(x) + \left(\frac{\hbar}{i}\right)^2 S_2(x) + \dots \quad (2)$$

Substituting this into the Schrödinger equation and collecting terms of equal powers of  $\hbar^2$  – gives recursive equations for the coefficients  $S_n(x)$ . The standard applicability condition of the WKB approximation requires that each subsequent term in this expansion be much smaller than the preceding one, i.e.,

$$\left| \frac{\hbar S_{n+1}(x)}{S_n(x)} \right| \ll 1. \quad (3)$$

For practical tunneling problems, this condition is equivalent to the requirement that the potential  $V(x)$  varies slowly on the scale of the electron wavelength, namely,

$$\left| \frac{\hbar k'(x)}{k^2(x)} \right| \ll 1. \quad (4)$$

Equation (1) ensures that the semiclassical wave function varies smoothly, and quantum interference between adjacent turning points is negligible. Under this condition, the first-order WKB term dominates, and higher-order corrections can safely be ignored.

In tunnel diodes, the potential barrier is formed by the built-in electric field  $F(x)$  arising from heavy doping. The potential variation near the depletion region can be expressed as

$$V(x) = qF(x)x + V_0 \quad (5)$$

so that

$$k(x) = \sqrt{\frac{2m^*}{\hbar^2} [E - qF(x)x - V_0]}. \quad (6)$$

For typical heavily doped GaN or GaAs tunnel diodes, the field gradient  $F'(x)$  is moderate and the characteristic spatial scale  $L = |V(x)/(dV/dx)|$  exceeds the de Broglie wavelength  $\lambda = 2\pi/k(x)$  satisfying Eq. (1) Therefore, the WKB approximation remains valid for calculating tunneling probabilities in such devices. This justification is consistent with the standard analysis presented by Karnakov and Krainov [14] and more recent works extending WKB theory to Dirac-like materials and two-dimensional tunneling systems [15,16].

Consequently, in the modeling of tunnel diodes presented in this paper, the first-order WKB term provides an accurate estimation of the transmission coefficient:

$$T(E) \approx \exp\left[-2 \int_{x_1}^{x_2} k(x) dx\right] \quad (7)$$

Where  $k(x) = \sqrt{\frac{2m^*}{\hbar^2} [V(x) - E]}$  is the imaginary wave number in the classically forbidden region. This formulation ensures that the WKB approximation is applied within its validity domain and that higher-order  $\hbar^2$ -corrections contribute negligibly to the total tunneling current. For the transmission coefficient, the following [14-16]:

$$P = \exp\left(-\frac{\alpha E_t^{\frac{3}{2}}}{F}\right) \quad (8)$$

For the transfer (tunneling) coefficient, we use the following formula, where  $F$  – is the internal electric field strength,  $E_t = E_g - qV + \mu_n + \mu_p$ ;  $\alpha = \theta \frac{4\sqrt{2m_e}}{3Fqh}$ ;  $\theta \approx 1$  ( $\theta$  – by employing these relations with the constant parameter of the Chynoweth model), we arrive at the following expression[1]. We assume that the internal electric field  $F$  – is constant in the range  $F \approx 10^3 - 10^4 \frac{V}{m}$ .

$$I_T = APT \left( \int_0^{\mu_n + \mu_p - qV} \left( \frac{1}{\exp\left(\frac{\varepsilon - \mu_n}{kT}\right) + 1} - \frac{1}{\exp\left(\frac{\varepsilon - \mu_n + qV}{kT}\right) + 1} \right) \sqrt{\varepsilon(qV_K - E_g - qV - \varepsilon)} d\varepsilon \right) \quad (9)$$

Now, using this expression and taking into account the diffusion current, we obtain the following expression for the I–V characteristic of the tunnel diode:

$$I = APT \left( \int_0^{\mu_n + \mu_p - qV} \left( \frac{1}{\exp\left(\frac{\varepsilon - \mu_n}{kT}\right) + 1} - \frac{1}{\exp\left(\frac{\varepsilon - \mu_n + qV}{kT}\right) + 1} \right) \sqrt{\varepsilon(qV_K - E_g - qV - \varepsilon)} d\varepsilon + I_0 \left( \exp\left(\frac{-qV}{kT}\right) - 1 \right) \right) \quad (10)$$

Based on the model presented by Chynoweth, the excess current in a tunnel diode can be expressed as follows [17,18]:

$$I_{CH} = D \cdot P = \int \frac{1}{\exp\left(\frac{\varepsilon - \mu_n}{kT}\right) + 1} - \frac{1}{\exp\left(\frac{\varepsilon - \mu_n + qV}{kT}\right) + 1} (1 - \exp(-\frac{E_1}{E_g - qV + \mu_n + \mu_p})) (1 - \exp(-\frac{E_2}{E_g - qV + \mu_n + \mu_p})) d\varepsilon \cdot \exp\left(-\frac{\theta \frac{4\sqrt{2m_e}}{3qh} (E_g - qV + \mu_n + \mu_p)^{\frac{3}{2}}}{F}\right) \quad (11)$$

Here, for the density of states  $D$ , we used the model proposed by Kan. Tunnel diodes are required to withstand large currents and, in some cases, high temperatures. To achieve this, it is advisable to employ either heavy doping of the semiconductor material or heterojunctions. As a result of these methods, numerous discrete energy levels are formed within the forbidden band. To simplify the calculations, we assumed the density of states to be unity. In this case, electrons from the conduction band of the n-type semiconductor can tunnel into the forbidden band of the p-type semiconductor, where they may first occupy the impurity energy levels, then emit a phonon and transition to other impurity states, and finally fall into the valence band. Alternatively, electrons may first emit a phonon, then be captured by impurity levels before transitioning into the valence band of the p-type semiconductor. This process leads to an increase in the minimum current observed in the I–V characteristics of tunnel diodes, i.e., the excess current. When light is absorbed in a semiconductor diode, electron–hole pairs (EHPs) are generated. Their flow contributes to the external circuit, producing a photocurrent denoted as  $-I_{ph}$ . When the diode is illuminated, each absorbed photon generates one electron–hole pair. If these carriers reach the contacts before recombining, they contribute to the current [19-21]. The incident light intensity on the diode is denoted by  $P_{in}$ . The energy of each photon is given by:

$$E = \frac{hc}{\lambda} \quad (12)$$

Photocurrent in a tunnel diode arises due to photon absorption and is proportional to the incident optical power. By relating the photon flux to the optical power and introducing the external quantum efficiency  $\eta$ , the photocurrent expression is derived as:

$$I_{ph} = q\eta \frac{P_{in}\lambda}{hc} \quad (13)$$

$\eta$  – external quantum efficiency ( $0 \leq \eta \leq 1$ ), that is, how many photons are converted into carriers,  $h$  — Planck's constant,  $c$  — the speed of light.

#### Phonon absorption ( $E_g - \hbar\omega$ ):

An electron absorbs phonon energy and thereby gains additional energy. As a result, even an electron that would typically be unable to overcome the barrier may participate in the tunneling process. This opens a new tunneling channel,

increasing the total current. In the band diagram, this corresponds to an electron originating from a lower-energy level, which, with the assistance of a phonon, is elevated to a higher state and then undergoes tunneling.

## RESULTS AND DISCUSSION

The expression for the total current of the tunnel diode, accounting for the photocurrent, is given by the following formula:

$$I = I_T + I_X + I_{dif} + I_{ph} \quad (14)$$

### Phonon emission ( $E_g + \hbar\omega$ ):

During tunneling, an electron emits a phonon, thereby losing part of its energy. As a result, the initial energy required for tunneling becomes higher. In this case, the number of electrons capable of tunneling decreases, and consequently, the total current is reduced. In the band diagram, an electron originating from a higher-energy state undergoes tunneling and, by emitting a phonon, transitions to a lower energy level [11-13,20-23]. If we supplement expression (7) given above with the corresponding additional terms, we obtain

$$I = APT \left( \int_0^{\mu_n + \mu_p - qV} \left( \frac{1}{\exp\left(\frac{\varepsilon - \mu_n}{kT}\right) + 1} - \frac{1}{\exp\left(\frac{\varepsilon - \mu_n + qV}{kT}\right) + 1} \right) \sqrt{\varepsilon(qV_K - E_g - qV - \varepsilon)} d\varepsilon + I_0 \left( \exp\left(\frac{-qV}{kT}\right) - 1 \right) \right. \\ \left. + \int \frac{1}{\exp\left(\frac{\varepsilon - \mu_n}{kT}\right) + 1} - \frac{1}{\exp\left(\frac{\varepsilon - \mu_n + qV}{kT}\right) + 1} \left( 1 - \exp\left(-\frac{E_1}{E_g - qV + \mu_n + \mu_p}\right) \right) \left( 1 - \exp\left(-\frac{E_2}{E_g - qV + \mu_n + \mu_p}\right) \right) d\varepsilon \cdot \right. \\ \left. \exp\left(-\frac{\theta^4 \sqrt{2me}}{3qh} (E_g - qV + \mu_n + \mu_p)^{\frac{3}{2}}\right) + q\eta \frac{P_{in}\lambda}{hc} \right) \quad (15)$$

The transmission coefficient of the tunnel diode when a phonon is absorbed  $P = \exp\left(-\frac{\alpha(E_t + \hbar\omega)^{\frac{3}{2}}}{F}\right)$ ; when emitting a phonon, it takes the form  $P = \exp\left(-\frac{\alpha(E_t - \hbar\omega)^{\frac{3}{2}}}{F}\right)$ .

Equation (15) represents the generalized current model of the tunnel diode, incorporating photocurrent contributions [16]. The total current of the tunnel diode is highly sensitive to incident optical flux and wavelength, with the photocurrent leading to a noticeable shift in the current–voltage characteristics. As the incident optical power ( $P_{in}$ ) increases, the photocurrent rises proportionally, directly shaping the diode's I–V curve. Figure 1 presents the calculated I–V characteristics for different illumination intensities ( $P_{in}$ ) and wavelengths ( $\lambda$ ). The plots illustrate the effects of incident optical power ( $P_{in} = 100$ –500 W/m<sup>2</sup>) and illumination wavelength ( $\lambda = 650$ –850 nm) on the total current, including cases where both tunneling and photocurrent contributions are included. The results indicate that an increase in optical flux enhances the overall current, while shorter wavelengths (corresponding to higher photon energies) improve the efficiency of the tunneling process.

The calculated three-dimensional I–V– $P_{in}$  characteristic of the tunnel diode is shown in Figure 2. The plots demonstrate that increasing optical intensity increases the photocurrent, shifting the total current surface.

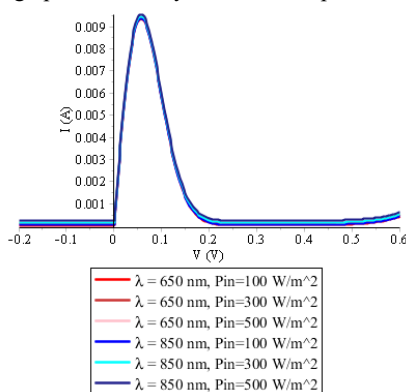


**Figure 1.** Calculated current–voltage characteristics of the tunnel diode under different optical excitation conditions.

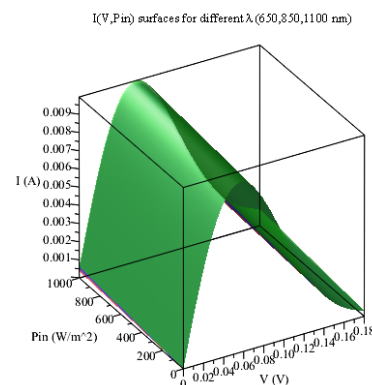


**Figure 2.** Three-dimensional current–voltage–optical power (I–V– $P_{in}$ ) surface characteristics of the tunnel diode for different wavelengths ( $\lambda = 650, 850, 1100$  nm).

The graph represents the sum of tunneling, diffusion, and photocurrent contributions for different wavelengths. As light intensity increases, the photocurrent rises, shifting the overall characteristic vertically. These findings confirm the strong optical sensitivity of tunnel diodes and highlight their potential for photodetection and advanced optoelectronic devices.

The current–voltage (I–V) characteristics of the p–n tunnel diode were measured both in complete darkness and under controlled optical illumination. In the absence of light, the dark current  $I_{dark}$  is dominated by direct band-to-band tunneling, enabled by the extremely high doping levels and the narrow depletion region characteristic of tunnel diodes.

Under illumination, the total current increases to

$$I_{\text{light}} = I_{\text{dark}} + I_{\text{ph}}$$

where  $I_{\text{ph}}$  is the optically generated photocurrent. At low and moderate biases, the illuminated I–V curve exhibits an approximately constant upward shift relative to the dark curve, corresponding to the bias-independent  $I_{\text{ph}}$ . At higher electric fields, especially near the resonant tunneling region, photocurrent alters both the peak and valley currents because the internal electric field distribution is modified. This effect is enhanced by field-dependent absorption due to the Franz-Keldysh effect, which changes the tunneling probability and therefore slightly modifies the Peak-to-Valley Ratio (PVR).

The photocurrent under monochromatic illumination of power  $P_{\text{opt}}$  –and photon energy  $h\nu$  is given

$$I_{\text{ph}} = q\eta \frac{P_{\text{in}}}{h\nu}$$

where  $q$  is the electron charge and  $\eta$  is the external quantum efficiency (EQE) of the device (fraction of incident photons producing collected carriers). Photosensitivity (responsivity) is defined as

$$S(\lambda) = \frac{I_{\text{light}} - I_{\text{dark}}}{P_{\text{opt}}}$$

In structures operating near the band edge, the Franz–Keldysh effect becomes significant. The enhanced electroabsorption leads to sub-bandgap optical response and shifts the spectral sensitivity curve toward longer wavelengths. As the bias increases, the absorption tail broadens, and oscillatory structures may appear due to modulation of the joint density of states [24–28].

To experimentally obtain the spectral response:

- The incident optical power  $P_{\text{opt}}(\lambda)$  is calibrated at each wavelength using a reference photodiode.
- The diode current is measured in darkness ( $I_{\text{dark}}$ ) and under monochromatic illumination ( $I_{\text{light}}(\lambda)$ ).
- The spectral responsivity is computed as

$$S(\lambda) = \frac{(I_{\text{light}}(\lambda) - I_{\text{dark}})}{P_{\text{opt}}(\lambda)}.$$

A plot of  $S(\lambda)$  vs.  $\lambda$  – reveals the Franz–Keldysh absorption tail below the nominal bandgap.

For a shot-noise-limited photodetector, the dominant noise source is the dark current. The noise current over a detection bandwidth  $\Delta f$  –is

$$\sigma_n = \sqrt{2qI_{\text{dark}}\Delta f}$$

The linear signal-to-noise ratio is

$$SRN_{\text{lin}} = \frac{I_{\text{ph}}}{\sigma_n} = \frac{I_{\text{light}} - I_{\text{dark}}}{\sqrt{2qI_{\text{dark}}\Delta f}}$$

In decibels:

$$SRN_{\text{dB}} = \frac{I_{\text{light}} - I_{\text{dark}}}{\sqrt{2qI_{\text{dark}}\Delta f}}.$$

Because tunnel diodes inherently exhibit high dark current, the corresponding shot noise is considerable. As a result, the signal-to-noise ratio (SNR) decreases with increasing bias voltage, which is consistent with the experimentally obtained SNR–V characteristics shown in Fig. 3 and Fig. 4. Although increasing bias enhances the photocurrent, it simultaneously increases  $I_{\text{dark}}$ , making an optimal operating bias essential.

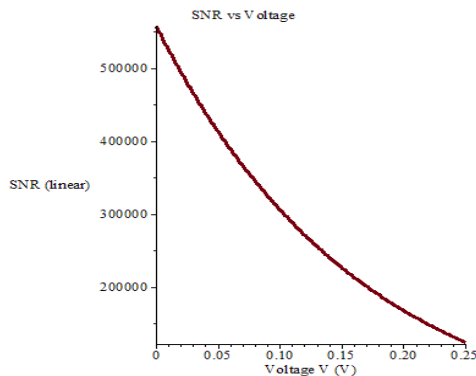


**Figure 3.** The measured current–voltage characteristic in complete darkness indicates tunneling-dominated conduction.

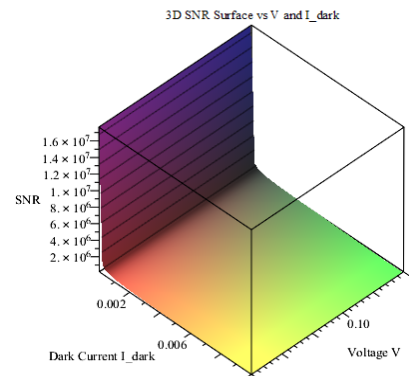


**Figure 4.** Three-dimensional mapping of the signal-to-noise ratio (SNR) dependence on the current–voltage ( $I_{\text{dark}}$ –V) characteristics.

## CONCLUSIONS

In this study, a unified theoretical model for the total current of a tunnel diode was developed. The model incorporates tunneling current, diffusion current, photocurrent, and the contribution of additional carriers generated through phonon interactions. This comprehensive formulation enables a clearer understanding of how optical excitation and phonon-assisted processes influence the tunneling mechanism.

The measured dark and illuminated I–V characteristics support the validity of the proposed model. In darkness, the current is governed by direct band-to-band tunneling, while under illumination the I–V curve exhibits a consistent upward shift due to the photocurrent. At higher electric fields, variations in the peak and valley currents arise from redistribution of the internal electric field and Franz–Keldysh-enhanced electroabsorption, leading to observable changes in the Peak-to-Valley Ratio (PVR). These graphical results confirm the strong interplay between tunneling, illumination, and internal field modulation.

Numerical simulations further demonstrate that changes in light intensity and phonon energy significantly affect the I–V behavior of tunnel diodes, particularly near the resonant tunneling region. These findings provide a solid theoretical basis for optimizing tunnel-diode-based photodetectors, high-speed optical switches, and low-power optoelectronic components.

Future work may extend the model by incorporating the Tien–Gordon framework and the effects of high-frequency electromagnetic fields, enabling a more detailed description of photon-assisted and RF-assisted tunneling phenomena.

## ORCID

✉ Mukhammadjon G. Dadamirzaev, <https://orcid.org/0000-0001-8258-4617>

✉ Munirakhon K. Uktamova, <https://orcid.org/0009-0005-7562-2677>

## REFERENCES

- [1] S.M. Sze, and K.K. Ng, *Physics of Semiconductor Devices*, (John Wiley & Sons, Inc., Hoboken, New Jersey, 2007). 3, 418 <https://onlinelibrary.wiley.com/doi/pdf/10.1002/9780470068328.fmatter>
- [2] E.O. Kane, “Zener tunneling in semiconductors,” *Journal of Physics and Chemistry of Solids* **12**, 181188 (1960). [https://doi.org/10.1016/0022-3697\(60\)90035-4](https://doi.org/10.1016/0022-3697(60)90035-4)
- [3] I. Shalish, “Franz-Keldysh effect in semiconductor built-in fields: Doping concentration and space charge region characterization,” *Journal of applied physics*, **124**, 075102 (2018). <https://doi.org/10.1063/1.5038800>
- [4] J.S. Karlovsky, “Simple Method for Calculating the Tunneling Current of an Esaki Diode,” *Phys. Rev.* **127**, 419 (1962). <https://doi.org/10.1103/PhysRev.127.419>
- [5] A.G. Chynoweth, W.L. Feldman, and R.A. Logan, “Excess Tunnel Current in Silicon Esaki Junctions,” *Phys. Rev.* **121**, 684 (1961). <https://doi.org/10.1103/PhysRev.121.684>
- [6] P.K. Tien, and J.P. Gordon, “Multiphoton Process Observed in the Interaction of Microwave Fields with the Tunneling between Superconductor Films,” *Physical Review*, **129**(2), 647–651 (1963). <https://doi.org/10.1103/PhysRev.129.647>
- [7] J.R. Tucker, “Quantum tunneling in electron devices,” *IEEE Journal of Quantum Electronics*, **15**(11), 1234-1252 (1979). <https://doi.org/10.1109/jqe.1979.1069931>
- [8] G. Gulyamov, and G. N. Majidova, “Influence of electron and phonon heating on the characteristics of solar photocells,” *Romanian Journal of Physics*, **68**(3–4), 607 (2023).
- [9] X. Liu, Q. Wang, L. Zhang, et al., “Analytical evaluation of tunneling current density in nonparabolic semiconductors,” *Physica Scripta*, **100**(4), 045503 (2025). <https://doi.org/10.1088/1402-4896/adeb06>
- [10] P. Février, M. Gabelli, et al., “Photon-assisted coherent transport in nanoscale tunnel junctions,” *Communications Physics*, **6**, 92 (2023). <https://doi.org/10.1038/s42005-023-01149-5>
- [11] J.P. Mendez, A. Torres, and D.F. de Lima, “Phonon-coupled tunneling in high-field quantum nanostructures,” arXiv preprint, arXiv:2410.17408, (2025). <https://arxiv.org/pdf/2410.17408>
- [12] T. Sugiura, Y. Morita, et al., “Analysis of tunneling mechanisms in renewable-energy semiconductor devices,” *Energy Science & Engineering*, **11**(10), 3888-3906 (2024). <https://doi.org/10.1002/ese3.1523>
- [13] B.M. Karnakov, and V.P. Krainov, *WKB Approximation in Atomic Physics*, (Springer, 2012). <https://doi.org/10.1007/978-3-031-60065-4>
- [14] V.A. Mishchenko, et al., “Generalized WKB theory for electron tunneling in gapped  $\alpha$ - $\beta$  lattices,” *Low Temperature Physics*, **51**, 588–595 (2025). <https://doi.org/10.1103/PhysRevB.103.165429>
- [15] G. Gulyamov, Sh.B. Utamuradova, M.G. Dadamirzaev, N.A. Turgunov, M.K. Uktamova, K.M. Fayzullaev, A.I. Khudayberdiyeva, et al., “Calculation of the Total Current Generated in a Tunnel Diode Under the Action of Microwave and Magnetic Fields,” *East European Journal of Physics*, (2), 221-227 (2023). <https://doi.org/10.26565/2312-4334-2023-2-24>
- [16] P.R. Berger, G. Gulyamov, M.G. Dadamirzaev, M.K. Uktamova, and S.R. Boidedaev, *Romanian Journal of Physics*, **69**, 609 (2024). <https://doi.org/10.59277/RomJPhys.2024.69.609>
- [17] A.G. Chynoweth, W.L. Feldman, and R.A. Logan, “Excess Tunnel Current in Silicon Esaki Junctions,” *Phys. Rev.* **121**, 684 (1961). <https://doi.org/10.1103/PhysRev.121.684>
- [18] T.A. Growden, M. Evan, D.F. Storm, P.R. Berger et al., 930 kA/cm<sup>2</sup> peak tunneling current density in GaN/AlN resonant tunneling diodes grown on MOCVD GaN-on-sapphire template, *Appl. Phys. Lett.* **114**, 203503 (2019).
- [19] I. Fistul, and N.Z. Shvarts, *Uspekhi Fizicheskikh Nauk*, **77**, 109–160 (1962).
- [20] M.W. Dashiell, J. Kolodzey, P. Crozat, F. Aniel, and J.M. Lourtioz, “Microwave properties of silicon junction tunnel diodes grown by molecular beam epitaxy,” *IEEE Electron Device Letters*, **23**, 357–359 (2002). <https://doi.org/10.1109/led.2002.1004234>
- [21] M. Lotfi, and D. Zohir, “International Journal of Control and Automation,” **9**(4), 9-50 (2016). <http://dx.doi.org/10.14257/ijca.2016.9.4.05>



- [22] Y. Yan, “Silicon-based tunnel diode technology,” Doctoral Thesis, University of Notre Dame, 2008.
- [23] P.R. Berger, in: *Comprehensive Semiconductor Science and Technology*, (2011), pp. 176–241. <https://doi.org/10.1016/B978-0-44-453153-7.00013-4>
- [24] Y. Turkulets, and I. Shalish, “Franz-Keldysh effect in semiconductor built-in fields: Doping concentration and space charge region characterization,” *Journal of Applied Physics*, **124**(7), 075102 (2018). <https://doi.org/10.1063/1.5038800>
- [25] Y.Wang, *et al.* “The influence of the Franz-Keldysh effect on the electron diffusion length in p-type GaN determined using the spectral photocurrent technique,” *Journal of Applied Physics*, **112**(4), 045401 (2012). <https://doi.org/10.1063/1.4746740>
- [26] C.Wang, *et al.* “Investigation of Franz–Keldysh effect in GaN-based structures by electroabsorption spectroscopy,” *Journal of Applied Physics*, **124**(3), 035703 (2018). <https://doi.org/10.1063/1.5031854>
- [27] R. Kudritzki, C. Zimmermann, and D. Feiler, “Illumination-induced modifications of tunneling current in heavily doped semiconductor junctions,” *Journal of Applied Physics*, **115**, 083704 (2014). <http://dx.doi.org/10.1063/1.4866852>
- [28] H.L. Hartnagel, and A. Pavlidis, “Bias-dependent photocurrent generation and tunneling enhancement in pn-junction-based photodetectors,” *Semiconductor Science and Technology*, **29**, 045007 (2014). <https://doi.org/10.1088/0268-1242/29/4/045007>

### МОДЕЛЮВАННЯ ВАХ-ХАРАКТЕРИСТИК ТУНЕЛЬНИХ ДІОДІВ З УРАХУВАННЯМ ФОТОСТРУМУ ТА ФОНОННИХ ПРОЦЕСІВ

Мухаммаджон Г. Дадамірзасв<sup>1</sup>, Мунірахон К. Уктамова<sup>1,2</sup>, Ширін Рахманова<sup>3</sup>, Гайрат А. Ібадуллаєв<sup>4</sup>

<sup>1</sup>Наманганський державний технічний університет, 160103 Наманган, Узбекистан

<sup>2</sup>Університет бізнесу та науки, Узбекистан

<sup>3</sup>Ургенчський державний університет, Узбекистан

<sup>4</sup>Ургенчський державний педагогічний інститут, Узбекистан

У цій статті розроблено єдину модель струму для тунельних діодів. Модель враховує не лише тунельний, дифузійний та надлишковий струми, але й фотострум, що генерується під час освітлення. Крім того, включено процеси тунелювання за допомогою фононів, а саме поглинання фононів та емісію фононів, що виникають внаслідок електрон-фононної взаємодії. Розраховані вольт-амперні характеристики показують, що загальний струм зміщується вниз під впливом освітлення. Показано, що фотострум зростає пропорційно оптичній інтенсивності та довжині хвилі. У випадку поглинання фононів електрони отримують додаткову енергію, тунельний канал розширюється, а піковий струм збільшується приблизно на 15–20%. І навпаки, під час емісії фононів частина енергії електронів втрачається, що зменшує ймовірність тунелювання, а піковий струм зменшується приблизно на 10–12%. Отримані результати показують, що врахування фононних та фотонних процесів значно розширює потенціал застосування тунельних діодів в оптоелектронних та фотодетекторних пристроях. Запропонована модель забезпечує теоретичну основу для розробки тунельних діодів як високочастотних, світлочутливих та енергоефективних пристроїв.

**Ключові слова.** тунельний діод; фотострум; дифузійний струм; надлишковий струм; моделювання напівпровідників; тунелювання за допомогою фононів; оптоелектронні пристрої